Contribution from the Departments of Chemistry, Hunter College, City University of New York, New York, New York 10021, and Colorado State University, Fort Collins, Colorado 80523

Structures and Properties of *N*-Methyltetraphenylporphyrin Complexes. Crystal and Molecular Structure and Cyclic Voltammetry of an Air-Stable Iron(II) Porphyrin: Chloro(*N*-methyl-5,10,15,20-tetraphenylporphinato)iron(II)

OREN P. ANDERSON,*[1] ALAN B. KOPELOVE,[2] and DAVID K. LAVALLEE*[2]

An air-stable iron(II) metalloporphyrin, chloro(*N*-methyl-5,10,15,20-tetraphenylporphinato)iron(II), has been characterized by cyclic voltammetry, and its crystal and molecular structures have been determined. Complexation with the coordinatively restrictive *N*-methylporphyrin ligand greatly stabilizes the Fe(II) oxidation state relative to Fe(III) ($E_{1/2}$ for [Fe(*N*-CH$_3$TPP)Cl] is +0.49 V vs. SCE while $E_{1/2}$ for [Fe(TPP)Cl] is −0.29 V). The cyclic voltammogram of the *N*-methylporphyrin complex shows reversible metal ion oxidation unlike the behavior of the nonmethylated porphyrin complex. The crystal and molecular structures of [Fe(*N*-CH$_3$TPP)Cl] have been determined from three-dimensional single-crystal X-ray diffraction data, collected by counter techniques. The dark blue crystals are triclinic, of space group $P\bar{1}$ (No. 2), with two formula units in the unit cell (a = 7.5620 (6) Å, b = 14.961 (2) Å, c = 17.434 (2) Å, α = 103.15 (1)°, β = 97.124 (9)°, γ = 93.84 (1)°). The structure has been refined by full-matrix least-squares methods to R = 0.043 (R_w = 0.055) for 4056 unique reflections with $F^2 > 3\sigma(F^2)$. The discrete, monomeric complexes exhibit a highly distorted square-pyramidal coordination geometry about the iron(II) atom, with the chloro ligand occupying the apical position (Fe–Cl = 2.244 (1) Å). The *N*-alkylated porphyrin ligand forms three strong bonds to the iron(II) atom (Fe–N2 = 2.118 (2) Å, Fe–N3 = 2.116 (2) Å, Fe–N4 = 2.082 (2) Å), together with one weaker bond (Fe–N1 = 2.329 (2) Å) between the methylated nitrogen atom and the iron(II) atom. The N1 binding energies indicate that the perturbation of the nitrogen atom due to the weaker bond is significant, however, for larger ions of the first transition series (Fe(II) and Mn(II)) and that this perturbation decreases with decreasing size, becoming insignificant for Zn(II).

Introduction

All iron(II) porphyrin complexes previously reported in the literature are readily oxidized by air. Earlier we demonstrated that complexation of manganous ion by an *N*-methylporphyrin (*N*-methyltetraphenylporphyrin or *N*-methyldeuteroporphyrin IX dimethyl ester) results in stabilization of the Mn(II) state relative to the Mn(III) state by nearly 1 V ($E_{1/2}$ = −0.23 V in chloro(tetraphenylporphinato)manganese(III) while $E_{1/2}$ = 0.76 V in chloro(*N*-methyltetraphenylporphinato)manganese(II)[3]). Similar stabilization for Fe(II) was anticipated, and the results of the synthesis, cyclic voltammetry, and molecular structure determination of the air-stable chloro(*N*-methyltetraphenylporphinato)iron(II), [Fe(*N*-CH$_3$TPP)Cl], are reported herein.

Experimental Section

Synthesis. Chloro(*N*-methyltetraphenylporphinato)iron(II), [Fe(*N*-CH$_3$TPP)Cl], was prepared by the addition of anhydrous FeCl$_3$ (0.24 mmol) and excess iron wire (0.50 mmol) to dry, distilled,[4] aerated THF (150 mL). The reaction mixture was refluxed under nitrogen for several hours, and *N*-methyltetraphenylporphyrin, prepared from CH$_3$SO$_3$F and TPP,[5] was added (0.16 mmol). The solution rapidly turned deep green. After the solution had cooled, a stoichiometric amount of a noncoordinating base, tetramethylpiperidine or 2,6-

lutidine, was added. The solution was filtered and allowed to evaporate. The product was repeatedly recrystallized from solutions of dichloromethane and acetonitrile. In solution, [Fe(*N*-CH$_3$TPP)Cl] is air stable but is readily demetalated by acid to form protonated porphyrin cations.

Cyclic Voltammetry was done in CH$_2$Cl$_2$ (dried over a 4-A molecular sieve) with 0.1 M tetrabutylammonium perchlorate (TBAP) recrystallized from methanol as supporting electrolyte. Solutions were deaerated with prepurified N$_2$ for 15 min prior to the measurements, and N$_2$ was passed over the solution during the analysis. A three-electrode system was used with a Bio-Analytical Systems CV-1A instrument and a Houston Model 2000 recorder. The working electrode was a Pt-button electrode, the auxiliary electrode was a Pt-wire coil, and a commercial aqueous saturated calomel electrode (SCE), separated from the sample solution by a fiber bridge, was used as the reference electrode. Potentials are reported relative to the aqueous SCE.

Crystal Data. For Fe(N$_4$C$_{45}$H$_{31}$)Cl: mol wt 719.07, triclinic, a = 7.5620 (6) Å, b = 14.961 (2) Å, c = 17.434 (2) Å, α = 103.15 (1)°, β = 97.124 (9)°, γ = 93.84 (1)°, V = 1896.6 Å^3, ρ_{calcd} = 1.26 g cm^{-3}, Z = 2, $F(000)$ = 744; space group $P\bar{1}$ (No. 2), Mo Kα radiation, λ_1 = 0.709 30 Å, μ(Mo Kα) = 5.2 cm^{-1}.

Data Collection and Reduction. Preliminary Weissenberg and precession photographs revealed only Laue symmetry $\bar{1}$, consistent with the triclinic crystal system. Because the structural studies of the other *N*-methylporphyrin complexes investigated in this series of papers have been completed by using the centrosymmetric space group $P\bar{1}$,[6–9] the same choice was made initially for the present work, and

(1) Colorado State University.
(2) Hunter College.
(3) D. K. Lavallee and M. J. Bain, *Inorg. Chem.*, **15**, 2090 (1976).
(4) D. D. Perrin, W. L. F. Armarego, and D. R. Perrin, "Purification of Laboratory Chemicals", Pergamon Press, London, 1966.
(5) D. K. Lavallee and A. E. Gebala, *Inorg. Chem.*, **13**, 2004 (1974).

(6) O. P. Anderson and D. K. Lavallee, *J. Am. Chem. Soc.*, **98**, 4670 (1976).
(7) O. P. Anderson and D. K. Lavallee, *J. Am. Chem. Soc.*, **99**, 1404 (1977).

the correctness of this choice is attested to by the successful refinement of the structural model reported below.

The small, dark blue crystal chosen for data collection was mounted on the Enraf-Nonius CAD-4 diffractometer,[10] in an orientation in which none of the final reduced cell axes were aligned with the diffractometer spindle axis. After centering, the diffractometer was used to locate a group of 25 reflections widely separated in reciprocal space. Centering of these reflections (for which $7° < \theta < 22°$) by the diffractometer provided precisely determined setting angles (at 20 ± 1 °C) from which auto-indexing and least-squares refinement of cell parameters generated the primitive triclinic unit cell reported above.

The intensities of 6668 unique reflections with $2° < \theta < 25°$ were measured by θ–2θ scans, employing Mo Kα radiation (graphite monochromator). The total scan range was 1.0° for all reflections. For each reflection to be measured, a rapid prescan (3.33 deg min^{-1}) of the reflection yielded counting results which allowed calculation of the ratio $\sigma(I)/I$. If this ratio was greater than 0.33, the reflection was flagged as weak, and the prescan results were accepted as final for that reflection. If this ratio was less than 0.33, on the other hand, the reflection was scanned again, with the scan speed for this final scan varying (from 3.33 to 0.5° min^{-1}) according to the strength of the reflection as determined by the prescan. Background was counted at positions ±25% beyond the ends of the intensity scan range, for a total time equal to half the scan time. All measured reflections gave counting rates that were within the linear range of the detector and counting chain.

The intensities of two control reflections (060 and $\overline{2}$06) were measured at intervals of 2 h of X-ray exposure of the crystal, and no systematic changes in the intensities of these two reflections during data collection were observed. A check of the setting angles for two reflections (060 and $\overline{3}$02) was done after each group of 100 reflections, and the results of these orientation controls showed that the position of the crystal was stable throughout the course of data collection. At the completion of data collection, Lorentz and polarization corrections were applied to the observed data. No absorption correction was applied to the data, due to the low absorption coefficient for Mo Kα radiation reported above and the small size of the data collection crystal (0.30 × 0.25 × 0.125 mm). Reflections for which $F^2 > 3\sigma(F^2)$ were taken to be observed, and the 4056 unique reflections that met this criterion were used in the subsequent refinement of the structure.

Refinement of the Structure. Since the primitive triclinic unit cell generated by the autoindexing program (see above) was very similar to the unit cells observed for two other compounds in this series,[6-8] all nonhydrogen atoms were initially placed in positions which corresponded to the final positions obtained for [Mn(N-CH$_3$TPP)Cl].[8] In the subsequent calculations, scattering factors for iron, chlorine, nitrogen, carbon, and spherically bonded hydrogen[11] were taken from ref 12, as were the anomalous dispersion coefficients $\Delta f'$ and $\Delta f''$ used for all nonhydrogen atoms.

With starting positions obtained as described above, all nonhydrogen atoms refined satisfactorily through two cycles of refinement in which isotropic thermal parameters were assigned to each atom. These calculations were followed by two cycles of full-matrix least-squares refinement in which all the nonhydrogen atoms of the molecule were allowed to take on anisotropic thermal parameters. At the conclusion of these two cycles, the hydrogen atoms of the phenyl rings were included in the structural model by placing them in calculated idealized positions 0.95 Å from carbon with isotropic thermal parameters (B_{iso} = 6.0 Å^2). Refinement of this model, maintaining anisotropic thermal parameters for all nonhydrogen atoms, continued until most calculated parameter shifts were less than 10% of the estimated standard deviations for the corresponding parameters. The largest calculated parameter shift was only 35% of the corresponding estimated standard deviation on this final cycle of refinement.

Table I. Fractional Atomic Coordinates

atom	x^a	y	z
Fe(II)	0.19926 (6)	0.17752 (3)	0.26096 (3)
Cl$^-$	0.0784 (1)	0.21178 (8)	0.37404 (6)
N1	0.5058 (4)	0.1930 (2)	0.3052 (2)
N2	0.2630 (3)	0.3059 (2)	0.2340 (2)
N3	0.2377 (4)	0.0356 (2)	0.2360 (2)
N4	0.0136 (4)	0.1460 (2)	0.1577 (2)
C5	0.5696 (5)	0.1726 (3)	0.2248 (2)
C11	0.5579 (4)	0.1310 (2)	0.3524 (2)
C12	0.6507 (5)	0.1817 (2)	0.4256 (2)
C13	0.6563 (5)	0.2746 (2)	0.4266 (2)
C14	0.5693 (4)	0.2831 (2)	0.3528 (2)
C21	0.4005 (5)	0.3729 (2)	0.2708 (2)
C22	0.3776 (5)	0.4558 (3)	0.2436 (2)
C23	0.2232 (5)	0.4393 (2)	0.1916 (2)
C24	0.1520 (5)	0.3456 (2)	0.1867 (2)
C31	0.1163 (5)	−0.0336 (2)	0.1891 (2)
C32	0.1750 (5)	−0.1226 (3)	0.1924 (2)
C33	0.3305 (5)	−0.1070 (3)	0.2433 (2)
C34	0.3691 (5)	−0.0083 (2)	0.2711 (2)
C41	−0.0663 (4)	0.2090 (2)	0.1224 (2)
C42	−0.2234 (5)	0.1638 (3)	0.0671 (2)
C43	−0.2350 (5)	0.0740 (2)	0.0692 (2)
C44	−0.0842 (4)	0.0623 (2)	0.1249 (2)
C1	0.5144 (5)	0.0351 (2)	0.3282 (2)
C2	−0.0399 (4)	−0.0218 (2)	0.1408 (2)
C3	−0.0054 (4)	0.3024 (2)	0.1356 (2)
C4	0.5404 (5)	0.3644 (2)	0.3290 (2)
C111	0.6333 (5)	−0.0210 (2)	0.3681 (2)
C112	0.5689 (6)	−0.0802 (3)	0.4119 (3)
C113	0.6848 (7)	−0.1302 (3)	0.4481 (3)
C114	0.8627 (6)	−0.1247 (3)	0.4407 (3)
C115	0.9276 (6)	−0.0665 (3)	0.3985 (3)
C116	0.8149 (5)	−0.0138 (3)	0.3629 (2)
C211	−0.1637 (4)	−0.1061 (2)	0.1013 (2)
C212	−0.2474 (6)	−0.1566 (3)	0.1459 (2)
C213	−0.3634 (6)	−0.2353 (3)	0.1091 (3)
C214	−0.3932 (5)	−0.2643 (3)	0.0281 (3)
C215	−0.3121 (5)	−0.2154 (3)	−0.0170 (2)
C216	−0.1972 (5)	−0.1363 (3)	0.0184 (2)
C311	−0.1030 (5)	0.3604 (2)	0.0885 (2)
C312	−0.0969 (5)	0.3459 (3)	0.0072 (2)
C313	−0.1784 (6)	0.4025 (3)	−0.0357 (2)
C314	−0.2659 (6)	0.4738 (3)	0.0014 (3)
C315	−0.2756 (6)	0.4875 (3)	0.0806 (3)
C316	−0.1952 (6)	0.4309 (3)	0.1245 (3)
C411	0.6635 (5)	0.4480 (2)	0.3713 (2)
C412	0.8428 (5)	0.4481 (3)	0.3660 (3)
C413	0.9588 (6)	0.5269 (3)	0.4039 (3)
C414	0.8940 (7)	0.6030 (3)	0.4473 (4)
C415	0.7166 (7)	0.6013 (3)	0.4538 (3)
C416	0.6008 (6)	0.5251 (3)	0.4155 (3)

^{a} Estimated standard deviations are given in parentheses.

The final R ($=[\sum \|F_o| - |F_c\|/\sum |F_o|]$) value was 0.043, while the final R_w ($=[\sum w(|F_o| - |F_c|)^2/\sum w(F_o^2)]^{1/2}$) value was 0.055. The error in an observation of unit weight was 1.70. The least-squares refinement program in the Enraf-Nonius structure determination computing package minimizes $\sum w(|F_o| - |F_c|)^2$, where F_o and F_c are the observed and calculated structure factor amplitudes, respectively, and w is the weight for each reflection [$w = (\sigma(F_o))^{-2}$]. The standard deviation, $\sigma(F_o)$, was derived from counting statistics, with the uncertainty parameter, g, taken to be 0.04.[13,14] No correction for secondary extinction was included in the calculations. The highest peak in the final difference Fourier map corresponded to 0.45 e Å^{-3}, and most peaks were much less than this value.

Final atomic positional parameters for all nonhydrogen atoms of [Fe(N-CH$_3$TPP)Cl] are reported in Table I. Table VII, a listing of the calculated hydrogen atom positions, and Table VIII, a listing of the anisotropic thermal parameters for the nonhydrogen atoms,

(8) O. P. Anderson and D. K. Lavallee, *Inorg. Chem.*, **16**, 1634 (1977).
(9) D. K. Lavallee, A. B. Kopelove, and O. P. Anderson, *J. Am. Chem. Soc.*, **100**, 3025 (1978).
(10) Data collection and all crystallographic computations were performed on the Enraf-Nonius CAD4 diffractometer with SDP computing package at the Kjemisk Institutt, University of Bergen, Bergen, Norway (see Acknowledgment).
(11) R. F. Stewart, E. R. Davidson, and W. T. Simpson, *J. Chem. Phys.*, **42**, 3175 (1965).
(12) "International Tables for X-ray Crystallography", Vol. IV, Kynoch Press, Birmingham, England, 1974.

(13) P. W. R. Corfield, R. J. Doedens, and J. A. Ibers, *Inorg. Chem.*, **6**, 197 (1967).
(14) O. P. Anderson, A. B. Packard, and M. Wicholas, *Inorg. Chem.*, **15**, 1613 (1976).
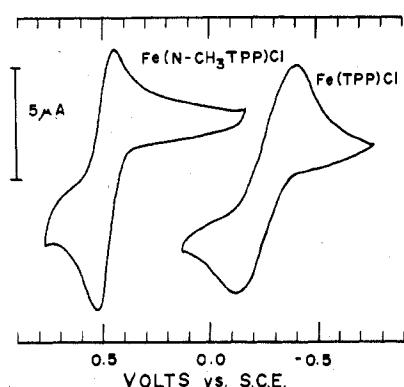
Figure 1. Cyclic voltammograms of [Fe(N-CH$_3$TPP)Cl] and [Fe-(TPP)Cl], each 1.0×10^{-3} M in CH$_2$Cl$_2$ with 0.10 M tetra-n-butylammonium perchlorate (TBAP) (scan rate 0.100 V/s).

are included with Table IX, a listing of the F_o and F_c values, as supplementary material.

Results and Discussion

All iron(II) porphyrin complexes reported to date undergo facile oxidation by air. Included among these complexes are, of course, the prosthetic groups of myoglobin, hemoglobin, and the cytochromes. We have been interested in the use of N-methylporphyrin complexes as spectroscopic and kinetic models for intermediates in porphyrin metalation,[15-17] but in addition we have found that they have remarkably different electrochemical properties from complexes of nonmethylated porphyrins—properties altered by constraints imposed on the coordination site.

Cyclic Voltammetry. Chloro(N-methyl-5,10,15,20-tetraphenylporphinato)iron(II) is air stable both in the solid state and in solution. The magnetic susceptibility of 5.2 μ_B (Faraday method) is characteristic of high-spin Fe(II),[18] consistent with previous characterization of [Mn(N-CH$_3$TPP)Cl] and [Co-(N-CH$_3$TPP)Cl] as high-spin species.[3] The cyclic voltammogram of [Fe(N-CH$_3$TPP)Cl] shows several one-electron processes as typically found for iron metalloporphyrin complexes. The cyclic voltammogram of [Fe(N-CH$_3$TPP)Cl] is qualitatively similar to that of [Fe(TPP)Cl], but it is quite possible that the processes giving rise to the certain peaks may be different in the two cases. From comparison of the cyclic voltammogram of [Fe(N-CH$_3$TPP)Cl] with that of [Zn(N-CH$_3$TPP)Cl] where the metal atom is not electroactive (which has $E_{1/2}$ values of 1.40, 1.10, −0.93, and −1.27 V) and in consideration of the reduced metal–ligand interaction in N-methylporphyrin complexes compared with complexes of nonmethylated porphyrins, we can assign the centermost peak to the Fe$^{3+/2+}$ process, and we assign the higher potential process at 1.51 V to N-methylporphyrin ligand oxidation and the two lower potential processes at −0.90 and −1.34 V to ligand reductions. Although we believe the tentative porphyrin ligand assignments to be reasonable, they contrast with assignments that have been made for iron complexes of nonmethylated porphyrins, in which Fe$^{4+/3+}$ and Fe$^{2+/1+}$ assignments have been made on the basis of the magnetic resonance spectra.[19,20] The largest and most interesting difference be-

Table II. Bond Lengths (Å) and Angles (Deg) Involving Fe(II)^a

(a) Bond Lengths

Fe(II)–Cl$^-$	2.244 (1)	Fe(II)–N3	2.116 (2)
Fe(II)–N1	2.329 (2)	Fe(II)–N4	2.082 (2)
Fe(II)–N2	2.118 (2)		

(b) Bond Angles

Cl$^-$–Fe(II)–N1	103.48 (6)	Fe(II)–N1–C5	98.0 (2)
Cl$^-$–Fe(II)–N2	105.36 (7)	Fe(II)–N1–C11	113.5 (2)
Cl$^-$–Fe(II)–N3	108.03 (7)	Fe(II)–N1–C14	112.7 (2)
Cl$^-$–Fe(II)–N4	114.38 (7)	Fe(II)–N2–C21	128.3 (2)
N1–Fe(II)–N2	82.18 (8)	Fe(II)–N2–C24	124.5 (2)
N1–Fe(II)–N3	82.25 (8)	Fe(II)–N3–C31	124.8 (2)
N1–Fe(II)–N4	142.13 (8)	Fe(II)–N3–C34	128.8 (2)
N2–Fe(II)–N3	145.60 (9)	Fe(II)–N4–C41	125.6 (2)
N2–Fe(II)–N4	87.12 (8)	Fe(II)–N4–C44	125.9 (2)
N3–Fe(II)–N4	86.64 (8)		

^{a} Estimated standard deviations are given in parentheses.

tween the cyclic voltammograms of [Fe(N-CH$_3$TPP)Cl] and those of other iron porphyrin complexes occurs in the intermediate potential region assigned to the Fe$^{3+/2+}$ process. This potential for [Fe(N-CH$_3$TPP)Cl] is 0.49 V vs. SCE while for [Fe(TPP)Cl], a high-spin five-coordinate complex, the corresponding process occurs at −0.29 V. The stabilization of the Fe(II) state relative to the Fe(III) state due to N-methylation of tetraphenylporphyrin (0.78 V) is nearly as great as the stabilization previously noted for Mn(II) in [Mn(N-CH$_3$TPP)Cl] vs. [Mn(TPP)Cl] (0.99 V, from −0.23 V in the TPP complex to 0.76 V in the N-CH$_3$TPP complex). The cyclic voltammograms in the Fe$^{3+/2+}$ region are illustrated in Figure 1. It should be noted that the Fe$^{2+/3+}$ process for the N-methylporphyrin is reversible (peak separation of 66 mV compared with 68 mV for ferrocene under the same conditions) whereas the corresponding process for [Fe(TPP)Cl] is highly irreversible. We observe peak separation of $\simeq$300 mV due to Cl$^-$ dissociation under our experimental conditions (see Figure 1). This separation is dependent on conditions (solvent, electrolyte, etc.) and scan rate. Values of $\simeq$100 mV and $\simeq$150 mV are reported by Kadish et al.[21]

For the sake of putting the magnitude of the change caused by N-methylation into perspective, we shall note comparisons that have been made for porphyrins with a variety of substituents and axial ligands. For the complexes [Fe(TPP)X] in CH$_2$Cl$_2$, the potentials are (X in parentheses) −0.47 (F$^-$),[22] −0.29 (Cl$^-$),[22] and −0.21 V (Br$^-$).[23] With the weakly binding ClO$_4^-$ as counterion, the potential for FeTPP$^+$ → FeTPP occurs at 0.14 V.[23] Some variation is also found within a series of iron porphyrin complexes with substituents in the para position of meso phenyl groups ([Fe(p-X)(TPP)Cl]). Iron reduction potentials in this series show a linear dependence on the Hammett σ constant of the para substituent with a reaction constant of only 0.04 in CH$_2$Cl$_2$ and even lower values in solvents of higher donor number (0.03 in DMF, 0.02 in DMA).[21] For a range of substituents from electron-withdrawing CN ($\rho = 0.66$) to electron-donating OCH$_3$ ($\rho = 0.27$) the total change in $E_{1/2}$ for the Fe$^{3+/2+}$ process is 0.15 V (in CH$_2$Cl$_2$).[21] Such substituents show a significantly larger effect on the porphyrin ligand oxidations and reductions (generally by a factor of 1.5–2). Substituent effects due to groups other than para phenyl substituents are available from data for the Fe$^{3+/2+}$ reductions of etioporphyrin I, octaethylporphyrin, deuteroporphyrin IX dimethyl ester, protoporphyrin IX, and tetraphenylporphyrin complexes: −0.34, −0.34, −0.34, −0.29,

(15) D. K. Lavallee, *Bioinorg. Chem.*, **6**, 291 (1976).
(16) D. K. Lavallee and M. J. Bain, *Bioinorg. Chem.*, **9**, 311 (1978).
(17) M. J. Bain-Ackerman and D. K. Lavallee, *Inorg. Chem.*, **18**, 3358 (1979).
(18) B. N. Figgis and J. Lewis, *Mod. Coord. Chem.*, 400 (1960).
(19) R. H. Felton, G. S. Owen, D. Dolphin, A. Forman, D. C. Borg, and J. J. Fajer, *Ann. N.Y. Acad. Sci.*, **206**, 504 (1973).
(20) D. Lexa, M. Momenteau, and J. Mispelter, *Biochim. Biophys. Acta*, **338**, 151 (1974).

(21) (a) K. M. Kadish, M. M. Morrison, L. A. Constant, L. Dickens, and D. G. Davis, *J. Am. Chem. Soc.*, **98**, 8387 (1976). (b) K. M. Kadish, J. S. Cheng, I. A. Cohen, and D. Summerville, *ACS Symp. Ser.*, No. **38**, 65 (1977).
(22) A. B. Kopelove and D. K. Lavallee, unpublished results.
(23) A. Wolberg, *Isr. J. Chem.*, **12**, 1031 (1974).
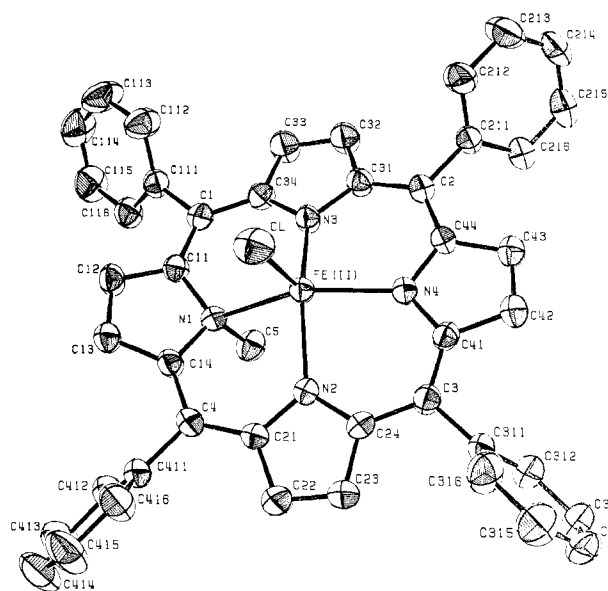
Figure 2. View of the [Fe(*N*-CH₃TPP)Cl] complex. Hydrogen atoms have been omitted for clarity, and the thermal ellipsoids have been drawn at the 50% probability level.

−0.27, and −0.18 V, respectively (DMF, Cl⁻ axial ligand).[24]

Considering the fact that the Fe–Cl bond length in [Fe-(*N*-CH₃TPP)Cl] is in the normal range for Fe(II) complexes, excluding a large effect of the axial ligand on $E_{1/2}$, and that the substituent effects on metal-centered reduction potentials noted above are much smaller than the effect due to N-methylation, we are drawn to a close inspection of the coordination site for an explanation of the large change on the $Fe^{3+/2+}$ potential.

Molecular Structure. Crystals of the compound [Fe(*N*-CH₃TPP)Cl] consist of discrete, neutral, monomeric complexes. Figure 2 shows the structure of one of these iron(II) *N*-methylporphyrin complexes, while Tables II and III contain the bond lengths and angles for this complex derived from the atomic coordinates reported above. Table IV contains the results of tests of the planarity of various parts of the *N*-methylporphyrin complex. Figure 3 displays the manner in which the molecular units are arrayed in the crystalline lattice as a result of the van der Waals and steric forces which control the lattice packing. No intermolecular interactions of any chemical significance were found to exist in the lattice.

The highly precise results obtained for [Fe(*N*-CH₃TPP)Cl] in this study reinforce and refine many of the conclusions reached in the earlier structural studies of the corresponding Co(II),[6,7] Mn(II),[8] and Zn(II)[9] *N*-CH₃TPP complexes. As was the case in these earlier studies, the coordination geometry about the metal atom is best described as a distorted square pyramid, with the four nitrogen atoms of the *N*-methyl-porphyrin ligand occupying the basal sites and the chloro ligand making a strong bond to the iron(II) atom from the apical position (Fe–Cl⁻ = 2.244 (1) Å). The rehybridization of the alkylated porphyrin nitrogen atom and the steric bulk of the *N*-methyl group lead to a large displacement of the metal ion above the reference plane of the three nonalkylated nitrogen atoms toward the apical chloro ligand. The 0.62-Å apical displacement of the iron(II) atom in the present study is comparable to the corresponding displacements seen in other *N*-CH₃TPP complexes (0.69 Å for Mn(II) in [Mn(*N*-CH₃-TPP)Cl],[8] 0.56 Å for Co(II) in [Co(*N*-CH₃TPP)Cl],[6,7] 0.65 Å for Zn(II) in [Zn(*N*-CH₃TPP)Cl][9]). This apical dis-

(24) K. M. Kadish and G. Larson, *Bioinorg. Chem.*, **7**, 95 (1977).
(25) A. Giraudeau, H. J. Callot, and M. Gross, *Inorg. Chem.*, **18**, 201 (1979).

Table III. Bond Lengths (Å) and Angles (Deg) for the *N*-Methylporphyrin Ligand[a]

(a) Bond Lengths

N1–C5	1.511 (3)	C1–C111	1.485 (4)
N1–C11	1.417 (3)	C111–C112	1.396 (4)
N1–C14	1.429 (3)	C112–C113	1.375 (5)
C11–C12	1.402 (4)	C113–C114	1.366 (6)
C12–C13	1.384 (4)	C114–C115	1.365 (6)
C13–C14	1.406 (4)	C115–C116	1.384 (4)
C11–C1	1.405 (4)	C116–C111	1.386 (4)
C14–C4	1.393 (4)	C2–C211	1.492 (4)
N2–C21	1.379 (3)	C211–C212	1.379 (4)
N2–C24	1.362 (3)	C212–C213	1.396 (5)
C21–C22	1.438 (4)	C213–C214	1.364 (5)
C22–C23	1.358 (4)	C214–C215	1.359 (5)
C23–C24	1.449 (4)	C215–C216	1.390 (4)
C21–C4	1.406 (4)	C216–C211	1.397 (4)
C24–C3	1.414 (3)	C3–C311	1.493 (4)
N3–C31	1.372 (3)	C311–C312	1.390 (4)
N3–C34	1.382 (3)	C312–C313	1.379 (4)
C31–C32	1.443 (4)	C313–C314	1.371 (5)
C32–C33	1.354 (4)	C314–C315	1.362 (6)
C33–C34	1.444 (4)	C315–C316	1.385 (5)
C31–C2	1.409 (4)	C316–C311	1.378 (5)
C34–C1	1.400 (4)	C4–C411	1.494 (4)
N4–C41	1.372 (3)	C411–C412	1.371 (4)
N4–C44	1.374 (3)	C412–C413	1.399 (4)
C41–C42	1.452 (4)	C413–C414	1.373 (6)
C42–C43	1.350 (4)	C414–C415	1.359 (6)
C43–C44	1.450 (4)	C415–C416	1.373 (5)
C41–C3	1.400 (4)	C416–C411	1.380 (5)
C44–C2	1.402 (4)		

(b) Bond Angles

C11–N1–C14	105.8 (2)	C2–C31–C32	123.5 (2)
C11–N1–C5	113.7 (2)	C31–C32–C33	106.9 (3)
C14–N1–C5	113.3 (2)	C32–C33–C34	107.0 (3)
N1–C11–C1	123.8 (2)	C33–C34–C1	124.1 (3)
N1–C11–C12	108.8 (2)	N3–C34–C33	110.0 (2)
C12–C11–C1	127.3 (3)	N3–C34–C1	125.9 (2)
C11–C12–C13	108.7 (2)	C34–C1–C111	120.1 (2)
C12–C13–C14	108.1 (2)	C11–C1–C111	115.7 (2)
C13–C14–N1	108.6 (2)	C34–C1–C11	124.2 (2)
C13–C14–C4	127.3 (3)	C1–C111–C112	122.2 (3)
N1–C14–C4	124.1 (2)	C111–C112–C113	119.9 (3)
C14–C4–C411	116.8 (2)	C112–C113–C114	121.2 (3)
C21–C4–C411	118.8 (2)	C113–C114–C115	119.4 (3)
C14–C4–C21	124.4 (2)	C114–C115–C116	120.6 (3)
C21–N2–C24	106.0 (2)	C115–C116–C111	120.4 (3)
N2–C21–C4	125.8 (2)	C116–C111–C1	119.4 (3)
N2–C21–C22	110.3 (2)	C116–C111–C112	118.4 (3)
C4–C21–C22	123.9 (3)	C2–C211–C212	120.7 (3)
C21–C22–C23	106.7 (3)	C211–C212–C213	120.8 (3)
C22–C23–C24	106.7 (3)	C212–C213–C214	120.2 (3)
C23–C24–N2	110.3 (2)	C213–C214–C215	120.0 (3)
C23–C24–C3	123.0 (2)	C214–C215–C216	120.8 (3)
N2–C24–C3	126.6 (2)	C215–C216–C211	120.1 (3)
C24–C3–C311	116.5 (2)	C216–C211–C2	121.2 (3)
C41–C3–C311	118.8 (2)	C216–C211–C212	118.2 (3)
C24–C3–C41	124.5 (2)	C3–C311–C312	120.2 (3)
C41–N4–C44	106.6 (2)	C311–C312–C313	120.4 (3)
N4–C41–C3	125.8 (2)	C312–C313–C314	120.3 (4)
N4–C41–C42	109.7 (2)	C313–C314–C315	119.8 (3)
C3–C41–C42	124.5 (2)	C314–C315–C316	120.6 (4)
C41–C42–C43	107.0 (2)	C315–C316–C311	120.3 (4)
C42–C43–C44	107.1 (2)	C316–C311–C3	121.2 (3)
C43–C44–N4	109.6 (2)	C316–C311–C312	118.6 (3)
C43–C44–C2	125.5 (2)	C4–C411–C412	119.0 (3)
N4–C44–C2	124.8 (2)	C411–C412–C413	119.6 (4)
C44–C2–C211	117.8 (2)	C412–C413–C414	120.2 (4)
C31–C2–C211	117.2 (2)	C413–C414–C415	119.7 (3)
C44–C2–C31	125.0 (2)	C414–C415–C416	120.6 (4)
C31–N3–C34	105.7 (2)	C415–C416–C411	120.5 (3)
N3–C31–C2	126.1 (2)	C416–C411–C4	121.6 (3)
N3–C31–C32	110.4 (2)	C416–C411–C412	119.4 (3)

[a] Estimated standard deviations are given in parentheses.

Table IV. Least-Squares Planes[a]

(a) Deviations from the Planes

plane 1 (n = 4) N1 (0.047), N2 (-0.048), N3 (-0.048),
N4 (0.048), Fe(II) (-0.665), C21 (-0.010), C22 (0.246),
C23 (0.332), C24 (0.134), C31 (0.138), C32 (0.400),
C33 (0.336), C34 (0.045), C41 (0.179), C42 (0.318),
C43 (0.281), C44 (0.139), C11 (-0.385), C12 (-1.081),
C13 (-1.119), C14 (-0.420), C1 (-0.172), C2 (0.147),
C3 (0.208), C4 (-0.241)
plane 2 (n = 3) N2, N3, N4, Fe(II) (-0.622), N1 (0.194),
C11 (-0.204), C12 (-0.846), C13 (-0.884), C14 (-0.239),
C21 (0.089), C22 (0.326), C23 (0.349), C24 (0.131),
C31 (0.135), C32 (0.416), C33 (0.416), C34 (0.144),
C41 (0.093), C42 (0.166), C43 (0.130), C44 (0.053),
C1 (-0.010), C2 (0.080), C3 (0.141), C4 (-0.079)
plane 3 (n = 5) N1 (0.000), C11 (-0.004), C12 (0.006),
C13 (-0.006), C14 (0.003), Fe(II) (-1.767), C5 (1.134),
C4 (-0.036), C1 (-0.061)
plane 4 (n = 5) N2 (0.011), C21 (-0.009), C22 (0.005),
C23 (0.002), C24 (-0.007), Fe(II) (-0.289), C3 (0.040)
C4 (-0.088)
plane 5 (n = 5) N3 (0.011), C31 (-0.010), C32 (0.006),
C33 (0.001), C34 (-0.008), Fe(II) (-0.211), C1 (-0.089),
C2 (0.017)
plane 6 (n = 5) N4 (-0.012), C41 (0.007), C42 (0.001),
C43 (-0.008), C44 (0.012), Fe(II) (-0.506), C2 (0.096),
C3 (0.054)
plane 7 (n = 6) C111 (0.008), C112 (0.003), C113 (-0.011),
C114 (0.008), C115 (0.004), C116 (-0.012), C1 (0.015)
plane 8 (n = 6) C211 (0.000), C212 (-0.003), C213 (0.006),
C214 (-0.004), C215 (0.000), C216 (0.002), C2 (-0.008)
plane 9 (n = 6) C311 (-0.011), C312 (0.004), C313 (0.006),
C314 (-0.009), C315 (0.003), C316 (0.008), C3 (-0.095)
plane 10 (n = 6) C411 (0.006), C412 (-0.010), C413 (0.004),
C414 (0.006), C415 (-0.010), C416 (0.004), C4 (0.025)

(b) Equations of the Planes[b]

plane	A	B	C	D
1	0.5938	0.0045	-0.8046	-2.4010
2	0.6308	0.0054	-0.7760	-2.2896
3	0.9265	0.0314	-0.3749	0.8815
4	0.6408	-0.1505	-0.7528	-2.7586
5	0.6135	0.1968	-0.7648	-2.3628
6	0.6789	-0.0144	-0.7341	-2.2159
7	-0.0148	-0.5602	-0.8282	-4.1649
8	-0.8165	0.5770	-0.0215	-0.0881
9	-0.7871	-0.5843	-0.1977	-2.1659
10	-0.0746	0.5741	-0.8154	-2.4129

(c) Dihedral Angles (Deg) between Selected Planes

planes	angle	planes	angle
1-2	2.7	2-5	11.0
1-3	31.6	2-6	3.8
1-4	9.8	2-7	50.9
1-5	11.3	2-8	-60.3
1-6	6.4	2-9	-69.7
1-7	49.1	2-10	53.9
1-8	-62.3	3-4	29.4
1-9	-71.9	3-5	30.5
1-10	52.1	3-6	25.3
2-3	28.9	4-5	20.1
2-4	9.1	4-6	8.2
		5-6	12.8

[a] In section a, numbers in parentheses refer to the distance (Å) of the given atom from the calculated plane. The first n atoms in each case determine the given plane. [b] In the form $Ax + By + Cz - D = 0$, where x, y, and z are orthogonalized coordinates (see D. M. Blow, *Acta Crystallogr.*, 13, 168 (1960)).

placement is much larger than the Fe···Cl distances of 0.42 and 0.40 Å seen in the nonalkylated five-coordinate high-spin porphyrin complexes [Fe(TPP)(2-MeIm)][26] and [Fe(TPivPP)(2-MeIm)][27] (where 2-MeIm is 2-methylimidazole,
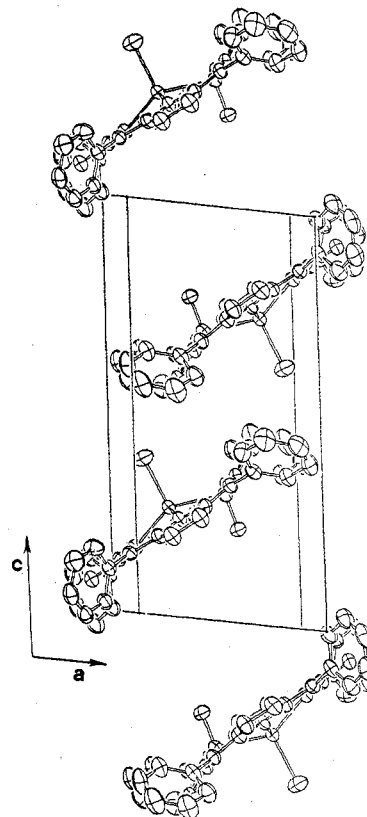
Figure 3. View (approximately down b) of the packing in the crystal lattice of [Fe(N-CH₃TPP)Cl].

Table V. Metal–Ligand Distances (Å) and Angles (Deg) in [M(N-MeTPP)Cl] Complexes[a]

	M(II)			
	Mn(II)[8]	Fe(II)	Co(II)[6,7]	Zn(II)[9]
M-Cl	2.295 (3)	2.244 (1)	2.243 (2)	2.232 (3)
M-N1	2.368 (5)	2.329 (2)	2.381 (5)	2.530 (7)
M-N2	2.155 (6)	2.118 (2)	2.063 (5)	2.089 (6)
M-N3	2.156 (5)	2.116 (2)	2.063 (5)	2.081 (9)
M-N4	2.118 (5)	2.082 (2)	2.016 (4)	2.018 (9)
N1-M-Cl	104.2 (1)	103.48 (6)	96.7 (1)	94.5 (2)
N4-M-Cl	118.6 (2)	114.38 (7)	116.6 (2)	120.8 (2)
N2-M-Cl	106.4 (1)	105.36 (7)	103.3 (1)	107.4 (2)
N3-M-Cl	109.6 (2)	108.03 (7)	105.9 (2)	105.6 (2)
M-N1-C11	111.4 (4)	113.5 (2)	113.6 (4)	108.8 (5)
M-N1-C14	110.9 (4)	112.7 (2)	112.7 (4)	107.9 (4)
M-N1-C5	99.7 (3)	98.0 (2)	96.1 (3)	94.1 (5)
C5-N1-C11	114.9 (5)	113.7 (2)	114.1 (5)	117.7 (6)
C5-N1-C14	114.3 (5)	113.3 (2)	114.1 (5)	118.5 (8)
C11-N1-C14	105.8 (5)	105.8 (2)	106.3 (5)	108.2 (8)

[a] Estimated standard deviations in parentheses.

and TPivPP is *meso*-tetrakis(*o*-pivalamidophenyl)porphyrin.

As can be seen in Table V, the metal–nitrogen bonds for the four N-CH₃TPP complexes which have now been studied follow a very similar pattern. In each case, only the bond from the metal to the nitrogen atom (N4) trans to the alkylated nitrogen atom (N1) is as short and as strong as similar bonds seen in "planar" (i.e., nonalkylated) porphyrin complexes. For example, the Fe-N4 distance of 2.082 (2) Å reported here is very similar to the Fe-N distances of 2.068 (5)–2.092 (4) Å reported for the [Fe(TPP)(2-MeIm)][26] and [Fe(TPivPP)(2-MeIm)][27] complexes mentioned earlier. The other two nonalkylated nitrogen atoms form slightly longer bonds to the

(26) J. L. Hoard in "Porphyrins and Metalloporphyrins", K. M. Smith, Ed., Elsevier, Amsterdam, 1975, p 317 ff.

(27) G. B. Jameson, F. S. Molinaro, J. A. Ibers, J. P. Collman, J. I. Brauman, E. Rose, and K. S. Suslick, *J. Am. Chem. Soc.*, 100, 6769 (1978).

Table VI. Delocalization Patterns (Å) in Porphyrins and *N*-Methylporphyrins

complex	nonmethylated pyrrole rings			methylated pyrrole rings		
	N-C$_a$	C$_a$-C$_b$	C$_b$-C$_b$	N-C$_a$	C$_a$-C$_b$	C$_b$-C$_b$
"planar" porphyrin^a	1.379 (6)	1.443 (5)	1.354 (10)			
Mn(*N*-MeTPP)Cl	1.373 (7)	1.448 (9)	1.356 (9)	1.424 (8)	1.406 (8)	1.398 (10)
Fe(*N*-MeTPP)Cl	1.374 (3)	1.446 (4)	1.354 (4)	1.423 (3)	1.404 (4)	1.384 (4)
Co(*N*-MeTPP)Cl	1.381 (8)	1.448 (9)	1.356 (9)	1.416 (8)	1.410 (9)	1.382 (9)
Zn(*N*-MeTPP)Cl	1.38 (1)	1.44 (1)	1.34 (2)	1.40 (1)	1.42 (2)	1.35 (1)

^{a} "Planar" here refers to a typical nonmethylated porphyrin (which may be "ruffled" to a considerable degree). Values presented on this line represent averaged bond lengths for 16 metalloporphyrins and are taken from Table II of ref 26. The nomenclature used here (C$_a$, C$_b$, etc.) is also described in this reference.

iron atom (Fe–N2 = 2.118 (2) Å, Fe–N3 = 2.116 (2) Å), just as was seen in the corresponding Mn(II), Co(II), and Zn(II) complexes. All of these distances are, of course, much longer than the Fe(II)–N distance of 1.972 (4) Å seen in the four-coordinate [Fe(TPP)] complex.[28]

The interaction between the iron(II) atom and the methylated nitrogen atom (N1) is much weaker than the other Fe–N bonds, as is evidenced by the Fe–N1 distance of 2.329 (2) Å seen here. The fact that all the Fe–N distances are approximately 0.04 Å shorter than the corresponding Mn–N distances in [Mn(*N*-CH$_3$TPP)Cl] is due to the smaller radius of the Fe(II) atom. This trend continues in the strong metal–nitrogen bonds (M–N2, M–N3, M–N4) of the [Co(*N*-CH$_3$TPP)Cl] complex, although the tendency of the cobalt(II) ion toward four-coordination leads to an actual lengthening of the very weak Co–N1 bond relative to the Fe(II) and Mn(II) cases. The tendency toward four-coordination reaches a maximum in the Zn(II) complex, where the Zn–N1 distance is roughly 0.2 Å longer than the Fe–N1 distance reported here. The extent of interaction between the metal atom and the nitrogen atoms to which it is bound can be estimated from the X-ray photoelectron spectra of these complexes in the N 1s binding energy region.[29] The changes in N 1s binding energies of the *N*-methyltetraphenylporphyrin ligand show that the perturbation of the N1 nitrogen compared to perturbation of the other three nitrogen atoms is about 50% for [Fe(*N*-CH$_3$TPP)Cl] (0.3 eV vs. 0.6 eV) compared with values of 70% for the larger Mn(II) atom (0.7 eV vs. 0.9 eV in [Mn(*N*-CH$_3$TPP)Cl]), about 40% for the smaller Co(II) atom (0.3 eV vs. 0.8 eV for [Co(*N*-CH$_3$TPP)Cl]), and only about 10% for the smallest atom investigated, Zn(II) (0.1 eV vs. 0.9 eV for [Zn(*N*-CH$_3$TPP)Cl]).[29] This weakening of the metal–nitrogen (M–N1) interaction as the propensity toward four-coordination grows is also reflected in the N1–M–Cl angle. This angle is about 104° in the two cases (Mn(II), Fe(II)) where the M–N1 interaction is strongest and drops to approximately 95° for the metal ions (Co(II), Zn(II)) for which this interaction is much less important. Further similarities between the coordination environments of the metal ions in these four *N*-CH$_3$TPP complexes and in the hybridization about the methylated nitrogen atom are made clear by the remaining values listed in Table V.

The entries in Table VI are designed to compare the bond lengths, and thus the effective delocalization patterns, within the pyrrole rings of the *N*-methylporphyrin ligands. In general, the bond lengths within the nonmethylated pyrrole rings are typical, in all four cases, of a normal "planar" porphyrin. The N–C and C–C bond distances in the methylated pyrrole ring are quite different, however, as a result of the change in hybridization at the N1 atom on methylation. The shift toward sp^3 character for this nitrogen atom on methylation results in N–C$_a$ bonds which are distinctly longer than the normal N–C$_a$

bonds of a "planar" porphyrin or the nonmethylated pyrrole rings in these *N*-CH$_3$TPP complexes. At the same time, the C$_a$–C$_b$ bonds for the methylated pyrrole ring are significantly shorter, in each case, than the corresponding bonds in nonmethylated pyrrole rings, while the C$_b$–C$_b$ bonds are generally significantly longer in the methylated pyrrole rings. Thus, the change in hybridization at N1 on methylation, with the concomitant large tilt of the N1 pyrrole ring relative to the N2–4 reference plane (dihedral angle approximately 30°), has a slight, but significant, effect on the pattern of delocalization in the pyrrole ring bonds. The changes seen are consistent with a decrease in delocalization through the methylated pyrrole ring. In this respect, the N–C$_a$ bonds would be seen to be longer as a result of the change toward sp^3 character at N1, the C$_a$–C$_b$ bonds become shorter (more like isolated double bonds), and the C$_b$–C$_b$ bonds become longer due to less effective delocalization of electrons involving these bonds.

Thus, the most striking structural differences between complexes of *N*-methyltetraphenylporphyrin and comparable (high-spin, five-coordinate) tetraphenylporphyrin complexes are the presence of one significantly weaker metal–nitrogen (M–N1) bond in the *N*-methylporphyrin complexes and the greater nonplanarity of the ligand (including the opposite sense of tilt for the methylated pyrrole ring). Both of these structural features can contribute to a greater stability of the reduced state relative to the oxidized state, i.e., a more favorable reduction potential. The effect of a difference in bonding is obviously relevant. Decreased planarity results in two effects that influence the reduction potential. Decreased planarity very likely leads to a smaller effective ligand field and less d orbital splitting. The smaller ligand field should provide less stabilization for the higher oxidation state of a metal ion. In addition, however, less effective dπ overlap is expected for the less planar *N*-methylporphyrin ligand. A smaller degree of dπ interaction is consistent with the similarity of visible absorption spectra of *N*-methylporphyrin complexes of a variety of metal ions compared with spectra of corresponding nonmethylated complexes[15,16] and with metal–chloride stretching frequencies of these *N*-methyltetraphenylporphyrin complexes which indicate that the metal ions behave more like typical complexes of hard ligands (e.g., CoCl$_4^{2-}$, MnCl$_4^{2-}$, etc.) than like the metal atoms in typical metalloporphyrins.[30] It would be expected that less dπ interaction would destabilize the back-bonding Fe(II) state relative to the Fe(III) state. It is quite possible that the opposing ligand field effect predominates. Further work with metal atoms of different d electron configuration and with different *N*-methylporphyrins is in progress to elucidate the relative importance of these factors.

(28) J. P. Collman, J. L. Hoard, G. Lang, L. J. Radonovich, and C. A. Reed, *J. Am. Chem. Soc.*, **97**, 2676 (1975).

(29) D. K. Lavallee, J. Brace, and N. Winograd, *Inorg. Chem.*, **18**, 1776 (1979).

(30) D. K. Lavallee, *Inorg. Chem.*, **17**, 231 (1978).

reported study. D.K.L. wishes to thank the donors of the Petroleum Research Fund, administered by the American Chemical Society, and gratefully acknowledges the PSC-BHE grant program of the City University of New York, for partial support of this work.

Contribution from the Department of Chemistry,
Brock University, St. Catharines, Ontario L2S 3A1, Canada

Reactions of Metal Ions with Vitamins. 2. Crystal Structures of Copper Complexes with Anionic and with Neutral Pyridoxamine[1]

KENNETH J. FRANKLIN and MARY FRANCES RICHARDSON*

Received January 30, 1980

The crystal structures of the two pyridoxamine (PM) complexes $Cu(PM)_2(NO_3)_2 \cdot H_2O$ ($CuC_{16}H_{26}N_6O_{11}$) and $Cu(PM-H)_2 \cdot 2H_2O$ ($CuC_{16}H_{26}N_4O_6$) have been determined from three-dimensional X-ray data collected by counter methods. $Cu(PM)_2(NO_3)_2 \cdot H_2O$ crystallizes in the triclinic space group $P\bar{1}$ with $Z = 2$ and cell dimensions $a = 14.248$ (2) Å, $b = 8.568$ (1) Å, $c = 9.319$ (1) Å, $\alpha = 94.08$ (1)°, $\beta = 89.73$ (1)°, and $\gamma = 99.13$ (1)°. The observed and calculated densities are both 1.61 g/cm^3. The structure was refined to a final R factor of 0.041 for 2390 observed reflections. The copper atoms lie on centers of symmetry and are chelated to the PM ligands through the 4-(aminomethyl) and phenolate groups of a PM zwitterion. Six-coordination is completed by nitrate groups, which bridge adjacent copper chelates through a single oxygen atom. $Cu(PM-H)_2 \cdot 2H_2O$ crystallizes in the orthorhombic space group $Pbca$, with cell dimensions $a = 10.982$ (1), $b = 13.918$ (1), and $c = 12.095$ (1) Å. The observed and calculated densities are 1.56 (1) and 1.57 g/cm^3, respectively, for $Z = 4$. The copper ions in this structure are also located on centers of symmetry and are chelated to the PM anions. Six-coordination of copper is completed by hydroxymethyl groups from neighboring molecules.

Introduction

Metal complexes of the B$_6$ vitamins and the Schiff bases derived from them have been an interesting area of study for the bioinorganic chemist.[2] Much research has been concerned with the liganding sites in these compounds.[3–14] In PM and PN, chelation though the 4-(aminomethyl) or 4-(hydroxymethyl) and phenolic groups has been suggested, whereas other experimental evidence points to bonding though the pyridine nitrogen or the side chains in the 5-position.[9–14] Chelation is always observed in the Schiff-base compounds.[15–22]

The question of binding site is complicated by the possibilities for tautomerism in the B$_6$ vitamins. For example, neutral PM has three tautomeric forms:
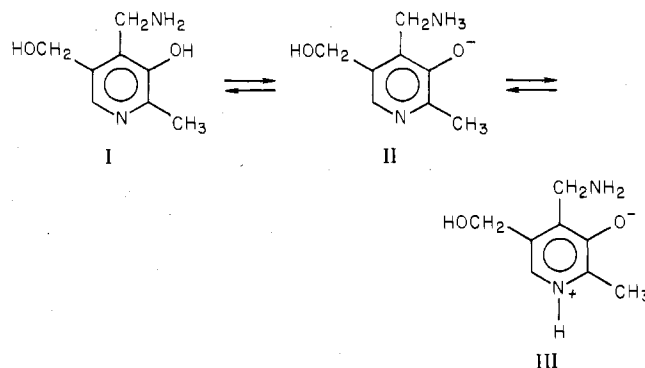
Tautomer II, which is the one actually found in crystalline PM and PM solutions,[23] is incapable of chelation because the amino group is protonated. Thus if chelation is to occur, one of the other two tautomers must be generated.

The two crystal structures reported herein for copper complexes of neutral and anionic PM show that chelation does in fact occur through the aminomethyl and phenolate groups of tautomer III and its anion. In addition, the hydroxymethyl

(1) For part 1 see M. F. Richardson, K. Franklin, and D. M. Thompson, *J. Am. Chem. Soc.*, **97**, 3204 (1975).
(2) R. H. Holm, *Inorg. Biochem.*, **2**, 1137–1167 (1973).
(3) R. L. Gustafson and A. E. Martell, *Arch. Biochem. Biophys.*, **68**, 485 (1957).
(4) M. E. Farago, M. M. McMillan, and S. S. Sabir, *Inorg. Chim. Acta*, **14**, 207 (1975).
(5) M. S. El-Ezaby and F. R. El-Eziri, *J. Inorg. Nucl. Chem.*, **38**, 1901 (1976).
(6) F. Gaillais, R. Haran, J. P. Laurent, and F. Nepveu-Juras, *C. R. Hebd. Seances Acad. Sci., Ser. C*, **284**, 29 (1977).
(7) K. J. Franklin and M. F. Richardson, *J. Chem. Soc., Chem. Commun.*, 97 (1978).
(8) A. Mosset, F. Nepveu-Juras, R. Haran, and J. J. Bonnet, *J. Inorg. Nucl. Chem.*, **40**, 1259 (1978).
(9) E. C. Kelusky and J. S. Hartman, *Can. J. Chem.*, **57**, 2118 (1979).
(10) T. S. Viswanathan and T. J. Swift, *Can. J. Chem.*, **57**, 1050 (1979).
(11) M. S. El-Ezaby and N. Gayed, *J. Inorg. Nucl. Chem.*, **37**, 1065 (1975).
(12) Ya. D. Fridman and M. G. Levina, *Russ. J. Inorg. Chem. (Engl. Transl.)*, **19**, 1324 (1974).
(13) M. S. El-Ezaby, M. Rashad, and N. M. Moussa, *J. Inorg. Nucl. Chem.*, **39**, 175 (1977).
(14) L. Asso, M. Asso, J. Mossoyan, and D. Benlian, *J. Chim. Phys. Phys.-Chim. Biol.*, **75**, 561 (1978).
(15) E. Willstadter, T. A. Hamor, and J. L. Hoard, *J. Am. Chem. Soc.*, **85**, 1205 (1963).
(16) J. F. Cutfield, D. Hall, and T. N. Waters, *Chem. Commun.*, 785 (1967).
(17) G. A. Bentley, J. M. Waters, and T. N. Waters, *Chem. Commun.*, 988 (1968).
(18) S. Yamada, Y. Kuge, T. Yamayoshi, and H. Kuma, *Inorg. Chim. Acta*, **11**, 253 (1974).
(19) S. Capasso, F. Giordano, C. Mattia, L. Mazzarella, and A. Ripamonti, *J. Chem. Soc., Dalton Trans.*, 2228 (1974).
(20) J. T. Wrobleski and G. L. Long, *Inorg. Chem.*, **16**, 2752 (1977).
(21) M. Nardelli, C. Pelizzi, and G. Predieri, *Transition Met. Chem.*, **3**, 233 (1978).
(22) M. Darriet, A. Cassaigne, J. Darriet, and N. Neuzil, *Acta Crystallogr., Sect. B*, **34**, 2105 (1978).
(23) O. A. Gansow and R. H. Holm, *Tetrahedron*, **24**, 4477 (1968).